ANL/NDM--63

DE82 009366

ANL/NDM-63

On Neutron Inelastic-Scattering Cross Sections of ^{232}Th, ^{233}U, ^{235}U, ^{238}U, ^{239}Pu and ^{240}Pu*

by

Alan B. Smith and Peter T. Guenther

January 1982

*This work supported by the U.S. Department of Energy.

Applied Physics Division
Argonne National Laboratory
9700 South Cass Avenue
Argonne, Illinois 60439
USA

NUCLEAR DATA AND MEASUREMENTS SERIES

The Nuclear Data and Measurements Series presents results of studies in the field of microscopic nuclear data. The primary objective is the dissemination of information in the comprehensive form required for nuclear technology applications. This Series is devoted to: a) measured microscopic nuclear parameters, b) experimental techniques and facilities employed in measurements, c) the analysis, correlation and interpretation of nuclear data, and d) the evaluation of nuclear data. Contributions to this Series are reviewed to assure technical competence and, unless otherwise stated, the contents can be formally referenced. This Series does not supplant formal journal publication but it does provide the more extensive information required for technological applications (e.g., tabulated numerical data) in a timely manner.

OTHER ISSUES IN THE ANL/NDM SERIES ARE:

ANL/NDM-1 Cobalt Fast Neutron Cross Sections-Measurement and Evaluation by P. T. Guenther, P. A. Moldauer, A. B. Smith, D. L. Smith and J. F. Whalen, July 1973.

ANL/NDM-2 Prompt Air-Scattering Corrections for a Fast-Neutron Fission Detector: $E_n \leq 5$ MeV by Donald L. Smith, September 1973.

ANL/NDM-3 Neutron Scattering from Titanium; Compound and Direct Effects by E. Barnard, J. deVilliers, P. Moldauer, D. Reitmann, A. Smith and J. Whalen, October 1973.

ANL/NDM-4 ^{90}Zr and ^{92}Zr; Neutron Total and Scattering Cross Sections by P. Guenther, A. Smith and J. Whalen, July 1974.

ANL/NDM-5 Delayed Neutron Data - Review and Evaluation by Samson A. Cox, April 1974.

ANL/NDM-6 Evaluated Neutronic Cross Section File for Niobium by R. Howerton, Lawrence Livermore Laboratory and A. Smith, P. Guenther and J. Whalen, Argonne National Laboratory, May 1974.

ANL/NDM-7 Neutron Total and Scattering Cross Sections of Some Even Isotopes of Molybdenum and the Optical Model by A. B. Smith, P. T. Guenther and J. F. Whalen, June 1974.

ANL/NDM-8 Fast Neutron Capture and Activation Cross Sections of Niobium Isotopes by W. P. Poenitz, May 1974.

ANL/NDM-9 Method of Neutron Activation Cross Section Measurement for E_n = 5.5-10 MeV Using the D(d,n)He-3 Reaction as a Neutron Source by D. L. Smith and J. W. Meadows, August 1974.

ANL/NDM-10 Cross Sections for (n,p) Reactions on ^{27}Al, $^{46,47,48}Ti$, $^{54,56}Fe$, ^{58}Ni, ^{59}Co and ^{64}Zn from Near Threshold to 10 MeV by Donald L. Smith and James W. Meadows, January 1975.

ANL/NDM-11 Measured and Evaluated Fast Neutron Cross Sections of Elemental Nickel by P. Guenther, A. Smith, D. Smith and J. Whalen, Argonne National Laboratory and R. Howerton, Lawrence Livermore Laboratory, July 1975.

ANL/NDM-12 A Spectrometer for the Investigation of Gamma Radiation Produced by Neutron-Induced Reactions by Donald L. Smith, April 1975.

ANL/NDM-13 Response of Several Threshold Reactions in Reference Fission Neutron Fields by Donald L. Smith and James W. Meadows, June 1975.

ANL/NDM-14 Cross Sections for the $^{66}Zn(n,p)^{66}Cu$, $^{113}In(n,n')^{113m}In$ and $^{115}In(n,n')^{115m}In$ Reactions from Near Threshold to 10 MeV by Donald L. Smith and James W. Meadows, July 1975.

ANL/NDM-15 Radiative Capture of Fast Neutrons in ^{165}Ho and ^{181}Ta by W. P. Poenitz, June 1975.

ANL/NDM-16 Fast Neutron Excitation of the Ground-State Rotational Band of ^{238}U by P. Guenther, D. Havel and A. Smith, September 1975.

ANL/NDM-17 Sample-Size Effects in Fast-Neutron Gamma-Ray Production Measurements: Solid-Cylinder Samples by Donald L. Smith, September 1975.

ANL/NDM-18 The Delayed Neutron Yield of ^{238}U and ^{241}Pu by J. W. Meadows January 1976.

ANL/NDM-19 A Remark on the Prompt-Fission-Neutron Spectrum of ^{252}Cf by P. Guenther, D. Havel, R. Sjoblom and A. Smith, March 1976.

ANL/NDM-20 Fast-Neutron-Gamma-Ray Production from Elemental Iron: $E_n \lesssim$ 2 MeV by Donald L. Smith, May 1976.

ANL/NDM-21 Note on the Experimental Determination of the Relative Fast-Neutron Sensitivity of a Hydrogenous Scintillator by A. Smith, P. Guenther and R. Sjoblom, June 1976.

ANL/NDM-22 Note on Neutron Scattering and the Optical Model Near A=208 by P. Guenther, D. Havel and A. Smith, September 1976.

ANL/NDM-23 Remarks Concerning the Accurate Measurement of Differential Cross Sections for Threshold Reactions Used in Fast-Neutron Dosimetry for Fission Reactors by Donald L. Smith, December 1976.

ANL/NDM-24 Fast Neutron Cross Sections of Vanadium and an Evaluated Neutronic File by P. Guenther, D. Havel, R. Howerton, F. Mann, D. Smith, A. Smith and J. Whalen, May 1977.

ANL/NDM-25 Determination of the Energy Scale for Neutron Cross Section Measurements Employing a Monoenergetic Accelerator by J. W. Meadows, January 1977.

ANL/NDM-26 Evaluation of the IN-115(N,N')IN-115M Reaction for the ENDF/B-V Dosimetry File by Donald L. Smith, December 1976.

ANL/NDM-27 Evaluated (n,p) Cross Sections of ^{46}Ti, ^{47}Ti and ^{48}Ti by C. Philis and O. Bersillon, Bruyeres-le-Chatel, France and D. Smith and A. Smith, Argonne National Laboratory, January 1977.

ANL/NDM-28 Titanium-II: An Evaluated Nuclear Data File by C. Philis, Centre d'Etudes de Bruyéres-le-Châtel, R. Howerton, Lawrence Livermore Laboratory and A. B. Smith, Argonne National Laboratory, June 1977.

ANL/NDM-29 Note on the 250 keV Resonance in the Total Neutron Cross Section of ^{6}Li by A. B. Smith, P. Guenther, D. Havel and J. F. Whalen, June 1977.

ANL/NDM-30 Analysis of the Sensitivity of Spectrum-Average Cross Sections to Individual Characteristics of Differential Excitation Functions by Donald L. Smith, March 1977.

ANL/NDM-31 Titanium-I: Fast Neutron Cross Section Measurements by P. Guenther, D. Havel, A. Smith and J. Whalen, May 1977.

ANL/NDM-32 Evaluated Fast Neutron Cross Section of Uranium-238 by W. Poenitz, E. Pennington, and A. B. Smith, Argonne National Laboratory and R. Howerton, Lawrence Livermore Laboratory, October 1977.

ANL/NDM-33 Comments on the Energy-Averaged Total Neutron Cross Sections of Structural Materials by A. B. Smith and J. F. Whalen, June 1977.

ANL/NDM-34 Graphical Representation of Neutron Differential Cross Section Data for Reactor Dosimetry Applications by Donald L. Smith, June 1977.

ANL/NDM-35 Evaluated Nuclear Data File of Th-232 by J. Meadows, W. Poenitz, A. Smith, D. Smith and J. Whalen, Argonne National Laboratory and R. Howerton, Lawrence Livermore Laboratory, February 1978.

ANL/NDM-36 Absolute Measurements of the $^{233}U(n,f)$ Cross Section Between 0.13 and 8.0 MeV by W. P. Poenitz, April 1978.

ANL/NDM-37 Neutron Inelastic Scattering Studies for Lead-204 by D. L. Smith and J. W. Meadows, December 1977.

ANL/NDM-38 The Alpha and Spontaneous Fission Half-Lives of ^{242}Pu by J. W. Meadows, December 1977.

ANL/NDM-39 The Fission Cross Section of ^{239}Pu Relative to ^{235}U from 0.1 to 10 MeV by J. W. Meadows, March 1978.

ANL/NDM-40 Statistical Theory of Neutron Nuclear Reactions by P. A. Moldauer, February 1978.

ANL/NDM-41 Energy-Averaged Neutron Cross Sections of Fast-Reactor Structural Materials by A. Smith, R. McKnight and D. Smith, February 1978.

ANL/NDM-42 Fast Neutron Radiative Capture Cross Section of ^{232}Th by W. P. Poenitz and D. L. Smith, March 1978.

ANL/NDM-43 Neutron Scattering from ^{12}C in the Few-MeV Region by A. Smith, R. Holt and J. Whalen, September 1978.

ANL/NDM-44 The Interaction of Fast Neutrons with ^{60}Ni by A. Smith, P. Guenther, D. Smith and J. Whalen, January 1979.

ANL/NDM-45 Evaluation of $^{235}U(n,f)$ between 100 KeV and 20 MeV by W. P. Poenitz, July 1979.

ANL/NDM-46 Fast-Neutron Total and Scattering Cross Sections of ^{107}Ag in the MeV Region by A. Smith, P. Guenther, G. Winkler and J. Whalen, January 1979.

ANL/NDM-47 Scattering of MeV Neutrons from Elemental Iron by A. Smith and P. Guenther, March 1979.

ANL/NDM-48 ^{235}U Fission Mass and Counting Comparison and Standardization by W. P. Poenitz, J. W. Meadows and R. J. Armani, May 1979.

ANL/NDM-49 Some Comments on Resolution and the Analysis and Interpretation of Experimental Results from Differential Neutron Measurements by Donald L. Smith, November 1979.

ANL/NDM-50 Prompt-Fission-Neutron Spectra of ^{233}U, ^{235}U, ^{239}Pu and ^{240}Pu Relative to that of ^{252}Cf by A. Smith, P. Guenther, G. Winkler and R. McKnight, September 1979.

ANL/NDM-51 Measured and Evaluated Neutron Cross Sections of Elemental Bismuth by A. Smith, P. Guenther, D. Smith and J. Whalen, April 1980.

ANL/NDM-52 Neutron Total and Scattering Cross Sections of ^{6}Li in the Few MeV Region by P. Guenther, A. Smith and J. Whalen, February 1980.

ANL/NDM-53 Neutron Source Investigations in Support of the Cross Section at the Argonne Fast-Neutron Generator by James W. Meadows and Donald L. Smith, May 1980.

ANL/NDM-54 The Nonelastic-Scattering Cross Sections of Elemental Nickel by A. B. Smith, P. T. Guenther and J. F. Whalen, June 1980.

ANL/NDM-55 Thermal Neutron Calibration of a Tritium Extraction Facility using the $^{6}Li(n,t)^{4}He/^{197}Au(n,\gamma)^{198}Au$ Cross Section Ratio for Standardization by M. M. Bretscher and D. L. Smith, August 1980.

ANL/NDM-56 Fast-Neutron Interactions with ^{182}W, ^{184}W and ^{186}W by P. T. Guenther, A. B. Smith and J. F. Whalen, December 1980.

ANL/NDM-57 The Total, Elastic- and Inelastic-Scattering Fast-Neutron Cross Sections of Natural Chromium, Peter T. Guenther, Alan B. Smith and James F. Whalen, January 1981.

ANL/NDM-58 Review of Measurement Techniques for the Neutron Capture Process by W. P. Poenitz, August 1981.

ANL/NDM-59 Review of the Importance of the Neutron Capture Process in Fission Reactors, Wolfgang P. Poenitz, (to be published).

ANL/NDM-60 Neutron Capture Activation Cross Sections of ^{94}, ^{96}Zr, $^{98,100}Mo$, and $^{110,114,116}Cd$ at Thermal and 30 keV Energy, John M. Wyrick and Wolfgang P. Poenitz, (to be published).

ANL/NDM-61 Fast-neutron Total and Scattering Cross Sections of ^{58}Ni by Carl Budtz-Jørgensen, Peter T. Guenther, Alan B. Smith and James F. Whalen, September 1981.

ANL/NDM-62 Covariance Matrices and Applications to the Field of Nuclear Data, by Donald L. Smith, Nobember 1981.

TABLE OF CONTENTS

ON NEUTRON INELASTIC-SCATTERING CROSS SECTIONS OF ^{232}Th, ^{233}U, ^{235}U, ^{238}U, ^{239}Pu and ^{240}Pu

by

Alan B. Smith and Peter T. Guenther
Applied Physics Divison
Argonne National Laboratory
9700 South Cass Avenue
Argonne, Illinois 60439
USA

ABSTRACT

Differential-neutron-emission cross sections of ^{232}Th, ^{233}U, ^{235}U, ^{238}U, ^{239}Pu and ^{240}Pu are measured between $\approx$ 1.0 and 3.5 MeV with the angle and magnitude detail needed to provide angle-integrated emission cross sections to $\lesssim$ 3% accuracies. Emitted-neutron resolutions are quantitatively defined and vary from $\approx$ 0.1 to 0.35 MeV. The experimental results are corrected for fission-neutron contributions to obtain pseudo-elastic-neutron-scattering cross sections which, together with the neutron total cross sections, define the non-elastic cross sections to within well specified energy resolutions. These results imply inelastic-neutron-scattering cross sections which are compared with comparable quantities derived from ENDF/B-V. Good general agreement is noted for ^{232}Th, ^{233}U, ^{235}U and ^{238}U inelastic-scattering values, poor agreement is observed for ^{240}Pu, and a serious discrepancy exists in the case of ^{239}Pu.

I. INTRODUCTORY REMARKS

Inelastic-neutron scattering from fissile and fertile targets has been of long-standing applied concern, particularly in the context of fast-breeder-reactor (FBR) systems[1]. Direct measurements of such processes in the fertile isotopes ^{232}Th and ^{238}U have led to partial understanding[2,3]. Similar measurements give fragmentary knowledge of inelastic-scattering processes in ^{240}Pu and very little information with respect to the fissile isotopes ^{233}U, ^{235}U and ^{239}Pu[4,5]. All of these direct measurements of inelastic scattering in the few-MeV region are complicated by the presence of fission neutrons and particularly so for the fissile targets where the fission cross sections can approach two barns. As a consequence of the limited experimental information, neutron-total-inelastic-scattering cross sections of the fertile targets in the few-MeV region are generally known to no better than 10% and to lesser accuracies in the fissile-target cases[2,3,5]. These uncertainties exceed the often quoted applied goals for neutron inelastic-scattering cross sections[1,6]. Appreciable improvement of the contemporary situation by direct inelastic-neutron measurement is difficult and tedious at best. Therefore, alternative approaches to the problem are sought.

Particularly as the result of recent measurements, neutron total cross sections of ^{232}Th, ^{233}U, ^{235}U, ^{238}U, ^{239}Pu, and ^{240}Pu are now known to $\lesssim$ 1 1/2% throughout the few-MeV region[7]. Steadily improving technologies suggest that pseudo-elastic-scattering measurements in the few-MeV region can now be made to accuracies which realistically permit determination of angle-integrated pseudo-elastic-scattering cross sections to uncertainties of $\lesssim$ 3% (herein "pseudoelastic" is defined as scattering due to E_x = 0.0 to some specified E_x = maximum). Fission cross sections of the fertile isotopes are relatively small and, for all six of the above isotopes, are known to $\lesssim$ 2-3%[2,3,8]. Nu-bar and its energy dependence is generally known to $\approx$ 2 1/2%. Neutron capture in the few-MeV region is relatively uncertain but generally very small. These observations suggest that a careful determination of the non-elastic-scattering cross sections and subsequent deduction of the implied inelastic-scattering cross sections could be productive. The measurements must deal with fission-neutron contamination but that perturbation is now more manageable as outlined below. The concept is not new[9] but contemporary accuracies in both magnitude and energy-resolution determinations give the approach new promise. An inspection of the relevant uncertainties suggests that a careful measurement of the pseudo-elastic-scattering cross sections could potentially define the total inelastic-scattering cross sections to within 5-10% for the excitation of all levels above $\approx$100 keV. In the MeV region, the excitation of lower-lying levels is usually of little applied consequence and their respective cross sections are frequently relatively small[8].

Following the above considerations, an attempt was made to determine the implied total-inelastic-scattering cross sections of ^{232}Th, ^{233}U, ^{235}U, ^{238}U, ^{239}Pu, and ^{240}Pu from $\approx$ 1 to 3.5 MeV with magnitude and energy definition sufficient to meet the needs of FBR applications. That attempt and the successful results are outlined below.

II. EXPERIMENTAL OUTLINE

A. Samples

A key factor in the measurements was the availability of an unusual, if not unique, set of samples. All the actinide samples were solid metal cylinders. The ^{232}Th, ^{235}U, ^{238}U, and ^{239}Pu samples were 2.0 cm in diameter and 2.0 cm high. The ^{233}U and ^{240}Pu samples were 2.00 and 1.89 cm high and 1.550 and 1.552 cm in diameter, respectively. The ^{233}U, ^{239}Pu, and ^{240}Pu samples were placed in 0.123 mm thick stainless-steel containers and identical containers were available for background determinations. Chemical impurities were negligible except for the ^{240}Pu sample which contained 0.8-1.0 weight/percent aluminum. The assay of this aluminum contaminant was based on weight and on neutron-transmission measurements,[10] and the ^{240}Pu experimental results were corrected using the aluminum cross sections of ref. 8. The ^{232}Th and ^{238}U samples were fabricated from elemental material. The ^{233}U sample was enriched to 99+ atom/percent in the primary isotope. The ^{235}U sample was enriched to 96 atom/percent in the primary isotope. The ^{239}Pu sample was enriched to 95.5 atom/percent in the primary isotope with the remaining material being essentially ^{240}Pu. The ^{240}Pu sample was enriched to 98 atom/percent with the remaining material being distributed among other Pu isotopes. Due to the high isotopic purities of the samples, corrections for minor-isotope contamination could be neglected except in the case of ^{235}U where small corrections were applied. The carbon calibration samples were fabricated from high-purity pile-grade graphite. The carbon-scattering sample was a cylinder 2.0 cm in diameter and 2.0 cm high. The carbon transmission samples were 2.54-cm-diameter discs of varying thicknesses selected to provide observed transmissions in the range of 0.4 to 0.75 at the particular measurement energy. Sample masses and dimensions were based upon precision physical measurements with accuracies of better than 1%.

B. Measurement Methods

All of the measurements were made using the Argonne National Laboratory ten-angle time-of-flight apparatus. Information about that apparatus and its application has been extensively reported elsewhere[11]. The relative energy dependencies of the ten primary neutron detectors were determined by the observation of neutrons emitted from the spontaneous fission of ^{252}Cf[12]. These relative response functions were correlated by observing neutrons scattered from carbon into each detector at a common scattering angle (nominally 30 deg.). The detector system was then used to determine the relative differential-elastic-scattering cross sections of carbon. These carbon measurements typically involved 80 differential values distributed between ≈ 16-160 deg. The neutron total cross sections of carbon were determined at identical incident energy and energy resolutions using conventional transmission techniques,[13] with attention to dead-time corrections. The statistical accuracies of the resulting carbon total cross sections were 1-2% and the results were generally consistent with those given in ENDF/B-V[8] to within the respective uncertainties. Care was

taken to avoid energies where the carbon total cross section is known to display prominent resonance structure. At the energies of the present work, the neutron total and elastic-scattering cross sections of carbon are essentially identical. Thus, the absolute normalization of the detector system was determined from the carbon total-cross-sections. Legendre-polynominal fits to the measured carbon relative-differential-elastic-scattering distributions were angle integrated and then normalized to the directly-measured neutron total cross sections. This normalization method is independent of any reference standard and implies measured differential-scattering cross sections relative to the measured carbon total cross sections. This method is not sensitive to the exact experimental energy scale or energy resolution.

The relative angular scale of the measurement system was optically determined to within $\approx \pm 0.2$ deg. The absolute normalization of this scale was fixed by observing neutrons scattered from bismuth and from hydrogen at a number of scattering angles on both sides of the apparent center line. The resulting absolute angular scale was thereby established to within $\approx \pm 0.5$ deg. This angular uncertainty is a concern in the present actinide measurements but significant improvements in the angular accuracy are difficult to achieve in a practical experimental environment.

The objective of the measurements was to obtain the actinide pseudo-elastic-scattering cross sections to the best possible accuracies, not the optimization of energy resolution. Thus, the resulting cross sections were inclusive of inelastic-neutron contributions corresponding to a specified excitation-energy range. This range varied from ≈ 0 to 90-350 keV and was defined to within ≈ 8 keV using the measured flight paths and time scales.

All measured differential-cross-section values were corrected for multiple event, beam-attenuation and angular-resolution perturbations using a combination of monte-carlo and analytical methods[14]. These correction procedures also gave detailed attention to fission-neutron contributions as discussed further below. The monte-carlo calculations were pursued to $\leq$ 1% precisions referenced to the angle-integrated cross-section results.

The sample-measurement sequence included actinide samples, background determinations (using empty containers if appropriate), and carbon scattering samples. The actinide samples, particularly ^{233}U and ^{240}Pu, were radioactive and their presence in the apparatus introduced an additional time-uncorrelated background. This latter background was essentially constant in time and thus was determined by normalization to regions of the observed time spectra forbidden to source-associated neutrons; e.g., to flight-time domains corresponding to neutron energies well below the actual detector response ranges.

C. Fission-neutron Corrections

Each of the actinide measurements included a fission-neutron component which made a large contribution to the measured values in some cases. The fission-neutron component was removed using two different correction methods.

In the first approach, a Maxwellian fission-neutron spectrum with a temperature T = 1.333 MeV was fitted to the higher-energy portion of the measured time-of-flight spectra; i.e., the portion above the elastic-scattering peak. These fitted fission-neutron spectral shapes were subtracted from the neutron-emission components defined within the specified scattered-neutron resolutions. The resulting fission-spectrum-subtracted values were corrected further for multiple-events, beam-attenuation, and angular-resolution effects as cited above. The final results were fully corrected differential pseudo-elastic-scattering cross sections including inelastically-scattered components up to a quantitatively defined excitation energy.

The second approach reduced the observed time-of-flight spectra to differential-neutron-emission cross sections inclusive of fission-neutron contributions and inelastic-scattering components within a well defined excitation-energy range. These emission cross sections were then corrected to obtain the pseudo-elastic-scattering cross sections using a monte-carlo simulation of the measurements. That simulation was based upon: the observed emission cross sections, the well-known neutron total and fission cross sections, and nubar (neutrons emitted per fission) and its energy dependence[15]. Fission-neutron spectra were assumed to have a Maxwellian form with a temperature T = 1.333 MeV. Inelastic neutron scattering corresponding to excitations beyond the experimental energy resolution was considered. Neutron capture cross sections are relatively very small and thus they were ignored. Otherwise, all aspects of the neutron interaction were given detailed attention. The requisite input parameters are known to good accuracies.

The two methods led to remarkably consistent pseudo-elastic-scattering results; the resulting angle-integrated cross sections frequently differ by less than 1%. The second, simulation, method was judged to be the more reliable as it was less sensitive to experimental statistical uncertainties. However, the results obtained using these methods generally imply inelastic-scattering cross sections differing by considerably less than the collective uncertainties attributable to other causes.

III. EXPERIMENTAL RESULTS

The measurements were made in approximately eight energy intervals distributed between $\approx$ 1.0 and 3.5 MeV and at $\geq$ 20 scattering angles in the range $\approx$ 16 to 160 deg. Two measurement periods were involved

providing considerable redundancy in the determination of the experimental values. Incident-neutron-energy resolutions were ≈ 50 to 70 keV. The well-defined scattered-neutron resolutions were larger and varied with target and incident-energy. Generally, they were selected to reflect known and prominent inelastic-scattering processes; e.g., the inelastic excitation of the ≈ 45 keV (2+) levels in ^{232}Th or ^{238}U was always included with the elastic-scattering component.

As outlined above, normalization of the actinide results was dependent upon the observation of differential-elastic scattering from carbon. Therefore, the carbon-scattering measurements were given careful attention. A representative experimental carbon result is shown in Fig. 1. Generally, and in this example, eighty differential-carbon values were obtained at each incident energy, representing four redundant values obtained at each of the 20 measurement angles. The statistical uncertainties of the measured values were generally $\lesssim$ 1% and the results were consistent to within the experimental uncertainties as illustrated in Fig. 1 where often the points obtained at a single angle are indistinguishable. The example of Fig. 1 is at an energy where the carbon distribution displays a prominent and well-known interference minimum,[16] this provides a physical verification of the angular scale of the measurement system. The angle-integrated carbon elastic scattering cross sections were determined by fitting the observed differential distributions with 6th-order Legendre series. Alternate choices of the order of the fit (e.g., 8th-order) led to similar angle-integrated cross sections (e.g., differing by fractional-percent amounts). The angle-integrated carbon elastic-scattering cross sections were related to the measured total cross sections to obtain the absolute normalization of the measurement system as outlined above.

Differential-scattered-neutron distributions for the six actinide samples were measured concurrently with the above carbon measurements. Generally, forty values were obtained for each sample and incident-energy, yielding sufficient redundancy at each scattering angle to test experimental consistency. The measured differential emission cross sections were corrected for multiple-events, beam-attenuation, angular resolution, backgrounds due to radioactivity, and fission-neutron contributions using the alternate procedures outlined above. The corrected results were pseudo-elastic-scattering cross sections inclusive of inelastically-scattered components corresponding to the excitation of levels up to an experimentally well defined low energy. Illustrative actinide angular distributions are shown in Fig. 2. The statistical accuracies of the individual differential values were generally $\lesssim$ 1%. Systematic uncertainties due to calibration and correction procedures were estimated to be 2-3%. The larger and denser samples with low radioactivity and small fission cross sections (e.g. ^{238}U) gave the best results. The values were less accurate for the smaller,

Fig. 1 Differential-elastic-scattering cross sections of carbon at an incident neutron energy of 3.55 MeV. Eighty measured values are indicated by data symbols which are often essentially superimposed. The curve is the result of a Legendre-series fit to the data. (dimensionality is b/sr and lab-deg.)

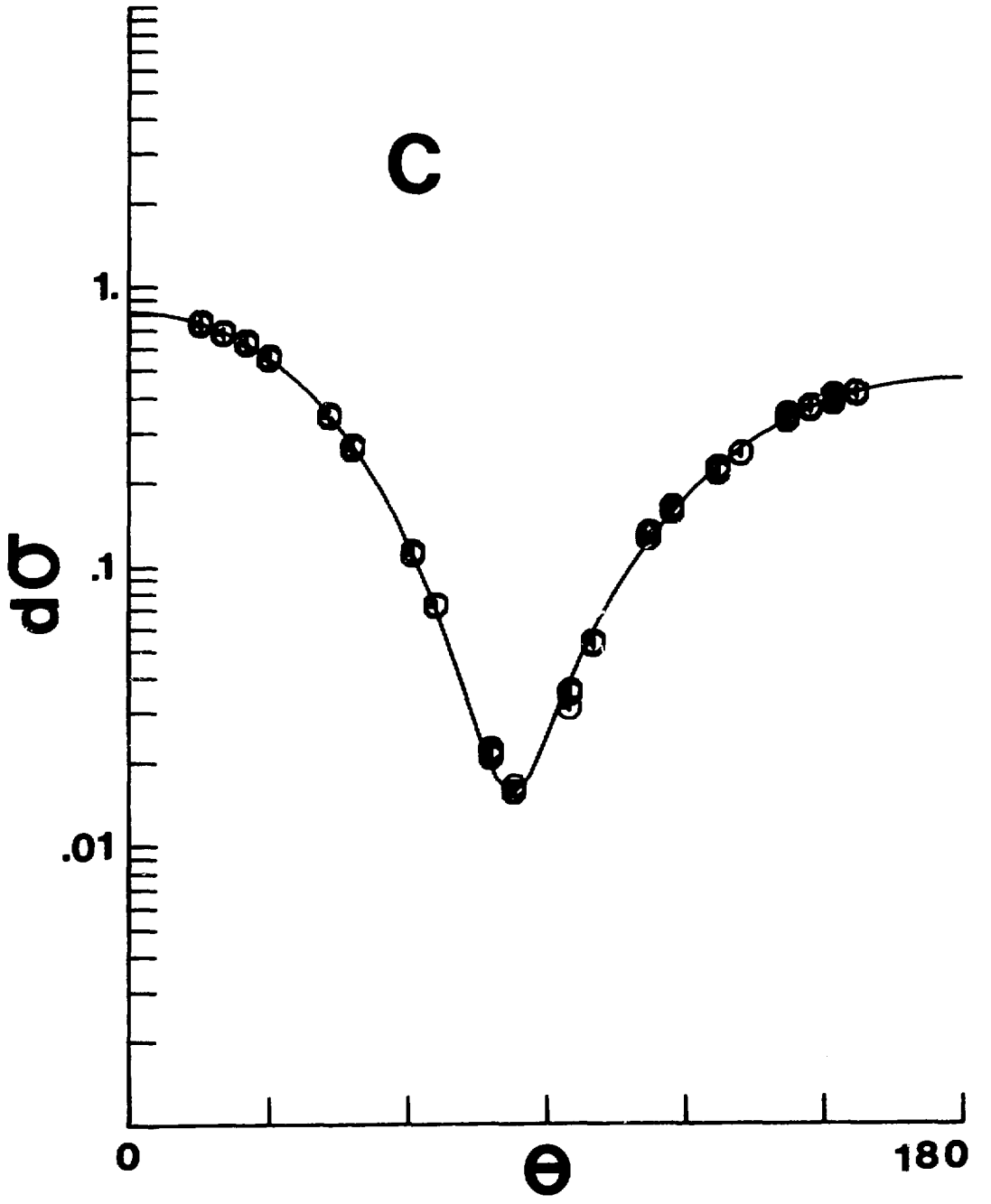
C
1.
.1
.01
dσ
0
θ
180

canned and very active samples with large fission cross sections (e.g., ^{233}U). Despite these latter problems, the neutron distributions obtained for all the actinide samples were well defined as illustrated in Fig. 2.

The present objective was the derivation of the implied inelastic-scattering cross sections, thus the emphasis was on the angle-integrated scattering cross section values. The latter were obtained by fitting the measured differential distributions with 8th-order Legendre series. The angle-integrated results were not particularly sensitive to the order of the Legendre series used in the fitting procedure. The quality of the fit to the measured data is illustrated in Fig. 2. The resulting angle-integrated cross sections were believed known to $\lesssim$ 3%. This uncertainty was dominated by uncertainties in detector calibration which were not correlated from measurement period to measurement period. Thus, it was gratifying to note that reproducibility was generally consistent with the above uncertainty estimates.

IV. DISCUSSION

The above pseudo-elastic-scattering cross sections imply inelastic scattering cross sections. The derivation required neutron total cross sections which were taken from work previously reported from this laboratory[7]. At the relevant energies, these total cross sections are known to $\lesssim$ 1 1/2% and consistent with previously reported results.[17] The necessary neutron-capture cross sections were taken from ENDF/B-V,[8] and a 10% uncertainty was assumed. The capture process has very little influence on the results. The interpretation also requires knowledge of the fission cross sections. The ^{232}Th and ^{238}U fission cross sections and associated uncertainties were taken from refs. 3 and 2, respectively. The ^{233}U and ^{235}U fission cross sections were taken from ENDF/B-V. The ^{235}U uncertainties were taken from the EMDF/B-V, and then it was assumed that the $^{233}U/^{235}U$ fission ratio was known to 1 1/2%. The ^{233}U fission cross section uncertainty was obtained from these two uncertainties. ^{239}Pu and ^{240}Pu fission cross sections, and associated uncertainties, were derived from the ratios to ^{235}U fission cross sections in a similar manner using the $Pu/^{235}U$ fission-cross-section ratios given in refs. 18 and 19, respectively. Generally, the fission cross sections derived in the above manner were consistent with those given in ENDF/B-V (identically so in the case of ^{235}U). The total-inelastic-scattering cross sections, above a well specified and low excitation energy, were obtained by combining the present experimental results with the above neutron total and partial cross sections. These are the inelastic-scattering cross sections that primarily influence energy transfer in FBR systems. The respective numerical values are set forth in Tables 1-A to F. The total-inelastic-scattering cross sections deduced from the present measurements are compared with the comparable quantities derived from ENDF/B-V in Fig. 3.

The present measurements imply ^{232}Th inelastic-scattering cross sections to $\approx$ 6-8% uncertainties except for the lowest-energy (0.93 MeV) value where the uncertainty is larger, since the difference between two

Fig. 2 Illustrative pseudo-elastic-scattering cross sections for ^{232}Th, ^{233}U, ^{235}U, ^{238}U, ^{239}Pu, and ^{240}Pu. The measured values are denoted by data symbols with 40 measurements per distribution. The curves indicate the results of Legendre-fits to the measured values. Incident energy in MeV is noted in each portion of the figure (dimensionality is b/sr and lab-deg.).

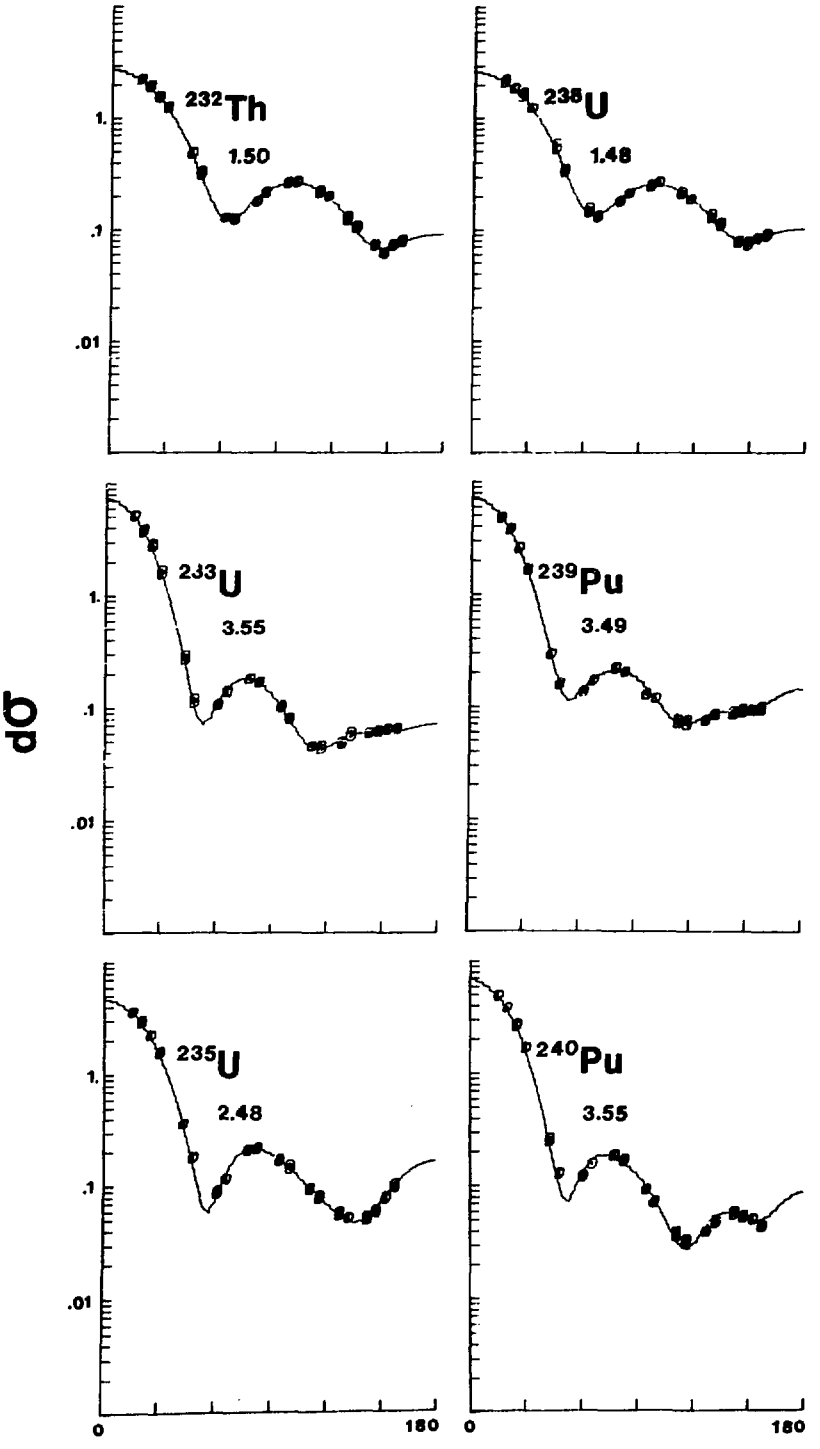
232Th
1.50
238U
1.48
233U
3.55
239Pu
3.49
235U
2.48
240Pu
3.55
1.
.1
.01
dσ
0
180
θ

large and similiar numbers is involved (see Table 1-A). Generally, the present inelastic-scattering results are in very good agreement with comparable values derived from ENDF/B-V as illustrated in Fig. 3. There is a discrepancy at the lowest measured energy. Here the measurements have a larger uncertainty, but it is noted that the value is very similiar to that obtained at the same energy for ^{238}U (see below) and the two nuclides are similiar. This suggests that the ENDF/B-V ^{232}Th evaluation underestimated the excitation of very low-lying levels at incident energies of $\approx$ 1 MeV; the information available for evaluation in this region was of marginal quality.

The present measurements imply the inelastic-scattering cross sections of ^{238}U to within 7-9%, again excepting the lowest-energy (0.93 MeV) value where the uncertainties are larger for the same reasons cited above (see Table 1-D). The present ^{238}U inelastic-scattering cross sections are in excellent agreement with the comparable quantities derived from ENDF/B-V as illustrated in Fig. 3.

The ^{235}U inelastic-scattering cross sections implied by the present measurements have uncertainties of 11-12% (see Table 1-C), again except for the low-energy 0.93 MeV value which is not as well known. 0.93 MeV is an unfortunate incident energy in the case of ^{235}U; it is near a region where the fission cross section changes rapidly with energy, and small variations in incident energy scale and/or resolution can significantly effect the inelastic-scattering result. This ^{235}U fission-cross-section uncertainty at $\approx$ 0.93 MeV may also be reflected in the ^{239}Pu results since the fission cross section of the latter isotope is often determined relative to that of ^{235}U. Otherwise, the ^{235}U inelastic-scattering cross sections deduced from the present measurements are in reasonably good agreement with those obtained from ENDF/B-V, as shown in Fig. 3. The consistency is generally within the uncertainties of the present measurements alone, and some uncertainty must be associated with the evaluation. This generally good agreement supports the previously described treatment of fission-neutron corrections since the ^{235}U fission cross sections are large throughout the energy range of the present measurements.

The uncertainties associated with the present ^{233}U inelastic-scattering results are $\approx$ 17-24% (see Table 1-B). These relatively large values reflect the very large fission cross section (and consequently small inelastic-scattering cross section) throughout the measured energy range. An additional experimental factor was the relatively high radioactivity of the samples. This particular case was the most difficult from the standpoint of fission-neutron corrections to the experimental observations. Despite these problems and uncertainties, the present experimental results are in very good agreement with those obtained from ENDF/B-V, as illustrated in Fig. 3.

The inelastic-scattering cross sections of ^{240}Pu derived from the present measurements are uncertain to $\approx$ 14-19% (see Table 1-F). These results are compared with corresponding quantities derived from ENDF/B-V in

Fig. 3 Neutron total-inelastic-scattering cross sections of ^{232}Th, ^{233}U, ^{235}U, ^{238}U, ^{239}Pu, and ^{240}Pu. Values deduced from the present measurements are noted by O. Comparable values derived from ENDF/B-V and the evaluation of ref. 21 are indicated by ■ and X, respectively. Curves are "eyeguides" referenced as follows; ——— present results, —— —— —— ENDF/B-V, and —— – – —— the evaluation of ref. 21.

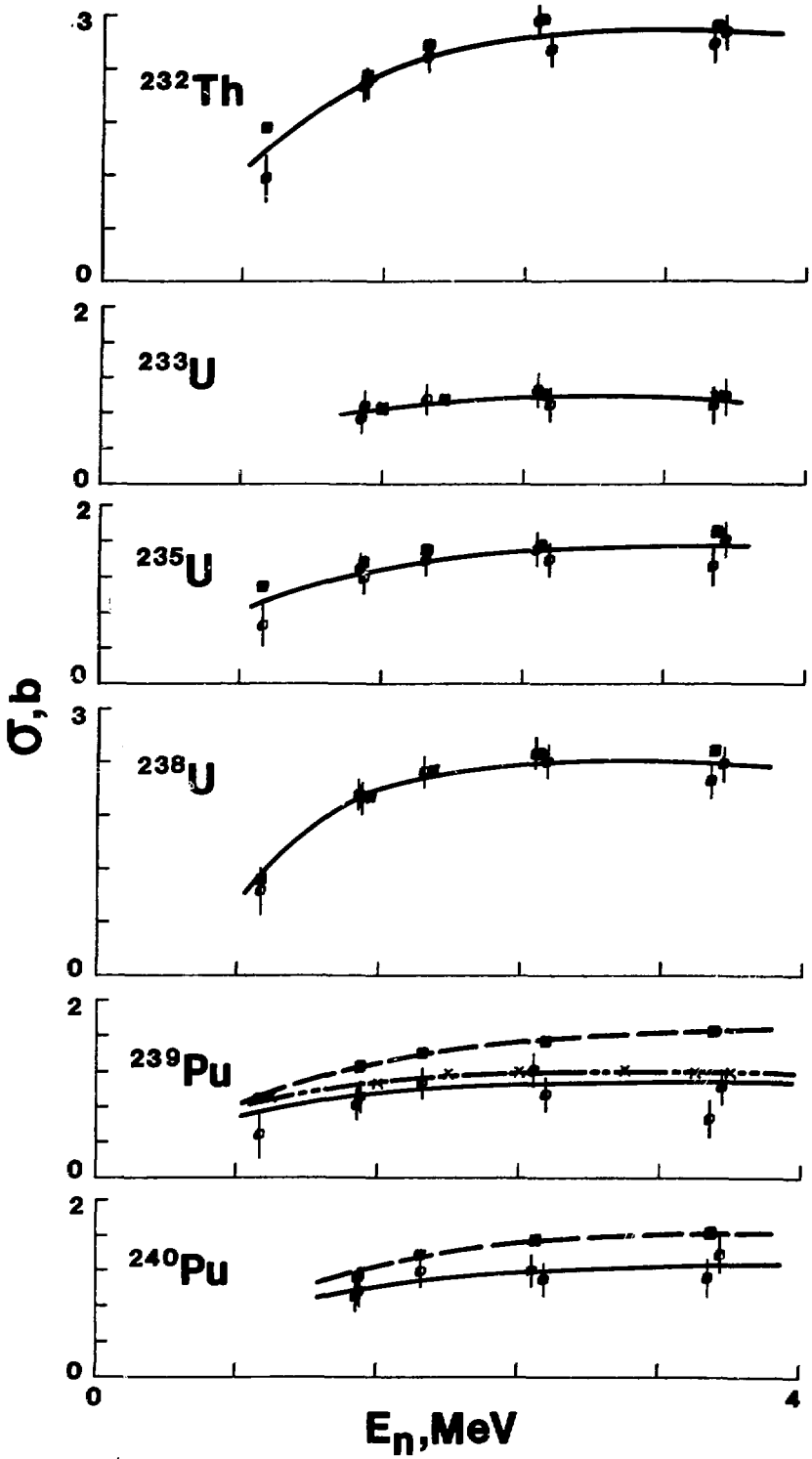
232Th
233U
235U
238U
239Pu
240Pu
σ,b
3
2
0
4
En,MeV

Fig. 3. The present results are ≈ 20-30% lower than those deduced from the File, and the discrepancy increases with energy. This discrepancy could be explained as a failure on the part of the evaluation to take proper account of the direct excitation of the low-lying levels of the ground-state-rotational-band of this even-even nucleus.

The ^{239}Pu inelastic-scattering cross sections deduced from the present measurements are uncertain to ≈ 15-20% (see Table 1-E). There are two exceptions: i) the suspect 0.93 MeV value noted above, and ii) what appears to be a somewhat anomalous experimental value at 3.48 MeV. Even given these uncertainties, the present ^{239}Pu inelastic-scattering results are 30-50% lower than implied by ENDF/B-V, as illustrated in Fig. 3. These are very large discrepancies in a cross section of an essential FBR material. It is difficult to attribute these discrepancies to experimental error. The other five nuclides were measured concurrently with ^{239}Pu, and the results for four of them are reasonably consistent with ENDF/B-V. The fission cross section of ^{239}Pu is no larger than that of ^{233}U, and the ^{233}U results are in good agreement with ENDF/B-V. Thus, the fission-neutron corrections seem to be suitable. The ^{239}Pu sample was large, with the consequence of good statistics, and the radioactive background was small. Moreover, ^{239}Pu and ^{233}U are similiar odd nuclei with similar total and fission cross sections and excited-level structure. Thus, one might expect somewhat similar inelastic-scattering cross sections. The present experimental results are consistent with that expectation; the ENDF/B-V evaluations are very different. In addition, the present experimental results are reasonably consistent with the results of calculations by Jary,[20] and with the values deduced from the evaluation of Antsipov et al.[21] as illustrated in Fig. 3.

In summary, the present work suggests that ^{232}Th, ^{233}U, ^{235}U, and ^{238}U total-inelastic-scattering cross sections over the incident energy range ≈ 1.0-3.5 MeV involving energy tranfers of more than several 100 keV as given in ENDF/B-V are correct to within the respective uncertainties. Thus, improvement in the understanding of inelastic scattering from these four nuclides should probably focus upon a better determination of energy transfer within an essentially fixed total-inelastic-scattering cross section. The present experiments also suggest that the inelastic-scattering cross sections of ^{239}Pu and ^{240}Pu as given in ENDF/B-V are too large by ≈ 30-50% and ≈ 20-30%, respectively. These are large discrepancies and, particularly in the case of ^{239}Pu, not consistent with frequently cited FBR accuracy goals.[1]

ACKNOWLEDGMENTS

The authors are indebted to personnel of the Applied Physics Divison, Argonne National Laboratory, for their assistance in these measurements and their interpretation.

REFERENCES

1. M. Salvatores, Proc. Specialist's Mtg. on Fast-Neut. Scattering on Actinide Nuclei, Paris (1981) to be published.

2. W. Poenitz, E. Pennington, A. Smith, and R. Howerton, Evaluated Fast-neutron Cross Sections of Uranium-238, Argonne Nat'l Lab. Report, ANL/NDM-32 (1977).

3. J. Meadows, W. Poenitz, A. Smith, D. Smith, J. Whalen, and R. Howerton, Evaluated Nuclear Data File of Th-232, Argonne Nat'l Lab. Report, ANL/NDM-35 (1978).

4. A. B. Smith, P. Lambropoulos, and J. F. Whalen, Nucl. Sci. and Eng., 47 19 (1972).

5. For example, Proc. Specialist's Mtg. on Fast-neut. Scattering on Actinide Nuclei, Paris (1981) to be published.

6. M. J. Lineberry, et al., "Reactivity Coefficients" Monograph on Current Status of Fast-Reactor Physics, to be published.

7. W. P. Poenitz, J. F. Whalen, and A. B. Smith, Nucl. Sci. and Eng., 78 333 (1981).

8. Evaluated Nuclear Data File-B, Version V, Brookhaven Nat'l Lab. Report, ENDF-201 (1979), compiled by R. Kinsey.

9. M. Walt, Proc. Conf. on Peaceful Uses of Atomic Energy, 2 18 United Nations Press, N.Y. (1955).

10. R. Gwin, private communication (1981).

11. For example, P. Guenther, D. Havel, and A. Smith, Fast-neutron Excitation of the Ground-state-rotational-band of U-238, Argonne Nat'l Lab. Report, ANL/NDM-16 (1975).

12. A. Smith, P. Guenther, and R. Sjoblum, Nucl. Instr. and Methods, 140 397 (1977).

13. D. Miller, Fast-neutron Physics, Vol. II, J. Marion and J. Fowler, Eds., Interscience Pub., New York (1963).

14. P. T. Guenther, Elastic and Inelastic Neutron Scattering from the Even Isotopes of Tungsten, Univ. of Illinois Thesis (1977).

15. R. J. Howerton, private communication (1981).

16. A. Smith, R. Holt, and J. Whalen, Neutron Scattering from C-12 in the Few-MeV Region, Argonne Nat'l Lab. Report, ANL/NDM-43 (1978).

17. For example, D. Foster and D. Glasgow, Phys. Rev., C3 576 (1971).

18. J. W. Meadows, Nucl. Sci. and Eng., 68 360 (1978).

19. J. W. Meadows, Nucl. Sci. and Eng., 79 233 (1981).

20. J. Jary, private communication (1981).

21. G. Antsipov, L. Bakhanovich, V. Zharkov, V. Zenevich, A. Klepatskii, V. Konshin, V. Maslov, G. Morogovskii, Yu. V. Porodzinskii, and E. Sh. Sukhovitskii, Nuclear Data Evaluation for Pu-239 in the Energy Range 10^{-5} eV - 15 MeV, International Atomic Energy Agency Report, INDC(CCP)-166/CHJ (1981).

Table 1-A, ^{232}Th Inelastic Scattering

A	B	C	D	E	F	G	H
E_n (MeV)	E_x (MeV)	σ_t (b)	σ_f (b)[c]	σ_c (b)[b]	σ_{scat} (b) = C-D-E	σ_{exp} (b)	σ_{inel} (b) = F-G
0.93	$\geq$ 0.09	7.10 $\pm$ .107[a] (7.05)[b]	0.0013 $\pm$ .0008	0.137 $\pm$ .014	6.962 $\pm$ .108	5.79 $\pm$ .231	1.171 $\pm$ .255[e] ($\pm$ 22%)
1.48	$\geq$ 0.18	6.90 $\pm$ .103[a] (6.89)[b]	0.064 $\pm$ .003	0.091 $\pm$ .009	6.745 $\pm$ .103	4.53 $\pm$ .136 (4.50)[d]	2.215 $\pm$ .171 ($\pm$ 7.7%)
1.50	$\geq$ 0.18	6.91 $\pm$ .104[a] (6.90)[b]	0.072 $\pm$ .003	0.091 $\pm$ .009	6.747 $\pm$ .104	4.50 $\pm$ .135 (4.50)[d]	2.247 $\pm$ .170 ($\pm$ 7.6%)
1.85	$\geq$ 0.18	7.14 $\pm$ .107[a] (7.06)[b]	0.089 $\pm$ .006	0.067 $\pm$ .007	6.984 $\pm$ .107	4.44 $\pm$ .133	2.544 $\pm$ .171 ($\pm$ 6.7%)
2.48	$\geq$ 0.30	7.58 $\pm$ .114[a] (7.48)[b]	0.115 $\pm$ .008	0.040 $\pm$ .004	7.425 $\pm$ .114	4.48 $\pm$ .134 (4.48)[d]	2.945 $\pm$ .176 ($\pm$ 6.0%)
2.55	$\geq$ 0.30	7.61 $\pm$ .114[a] (7.53)[b]	0.116 $\pm$ .008	0.040 $\pm$ .004	7.454 $\pm$ .114	4.84 $\pm$ .145 (4.80)[d]	2.614 $\pm$ .184 ($\pm$ 7.0%)
3.48	$\geq$ 0.35	8.05 $\pm$ .121[a] (7.90)[b]	0.144 $\pm$ .006	0.023 $\pm$ .002	7.883 $\pm$ .121	5.21 $\pm$ .156 (5.22)[d]	2.673 $\pm$ .197 ($\pm$ 7.4%)
3.55	$\geq$ 0.35	8.05 $\pm$ .121[a] (7.90)[b]	0.144 $\pm$ .006	0.023 $\pm$ .002	7.883 $\pm$ .121	5.08 $\pm$ .152 (5.08)[d]	2.803 $\pm$ .194 ($\pm$ 6.9%)

[a]Taken from W. Poenitz et al., ref. 7.

[b]Taken from ENDF/B-V, ref. 8.

[c]Taken from ANL/NDM-35, ref. 3.

[d]Taken from stripped spectra, see text.

[e]Errors combined in quadrature.

Table 1-B, ^{233}U Inelastic Scattering

A	B	C	D	E	F	G	H
E_n (MeV)	E_x (MeV)	σ_t (b)[a]	σ_f (b)[b]	σ_c (b)[b]	σ_{scat} (b) = C-D-E	σ_{exp} (b)	σ_{inel} (b) = F-G
1.48	$\geq$ 0.13	6.75 $\pm$ .101 (6.748)[b]	1.904 $\pm$ .051[c]	0.032 $\pm$ .003	4.814 $\pm$ .113	4.08 $\pm$ .122 (3.98)[d]	0.734 $\pm$ .166 ($\pm$ 22.6%)
1.50	$\geq$ 0.13	6.76 $\pm$ .101 (6.788)[b]	1.907 $\pm$ .051[c]	0.032 $\pm$ .003	4.821 $\pm$ .113	3.94 $\pm$ .118 (3.92)[d]	0.881 $\pm$ .163 ($\pm$ 18.5%)
1.85	$\geq$ 0.18	7.06 $\pm$ .106 (7.041)[b]	1.940 $\pm$ .052[c]	0.019 $\pm$ .002	5.101 $\pm$ .118	4.15 $\pm$ .125 (4.04)[d]	0.951 $\pm$ .172 ($\pm$ 18.1%)
2.48	$\geq$ 0.30	7.53 $\pm$ .113 (7.551)[b]	1.922 $\pm$ .061[c]	0.0075 $\pm$ .0008	5.600 $\pm$ .128	4.54 $\pm$ .136 (4.46)[d]	1.061 $\pm$ .187 ($\pm$ 17.6%)
2.55	$\geq$ 0.30	7.56 $\pm$ .113 (7.595)[b]	1.914 $\pm$ .061[c]	0.0075 $\pm$ .0008	5.639 $\pm$ .128	4.75 $\pm$ .143 (4.57)[d]	0.889 $\pm$ .191 ($\pm$ 21.6%)
3.48	$\geq$ 0.35	8.02 $\pm$ .120 (7.925)[b]	1.779 $\pm$ .056[c]	0.0023 $\pm$ .0002	6.239 $\pm$ .132	5.36 $\pm$ .161 (5.29)[d]	0.879 $\pm$ .208 ($\pm$ 23.7%)
3.55	$\geq$ 0.35	8.02 $\pm$ .120 (7.93)[b]	1.768 $\pm$ .056[c]	0.0023 $\pm$ .0002	6.258 $\pm$ .132	5.28 $\pm$ .156 (5.08)[d]	0.978 $\pm$ .204 ($\pm$ 20.9%)

[a]Taken from W. Poenitz et al., ref. 7.

[b]Taken from ENDF/B-V, ref. 8.

[c]Assuming ^{235}U uncertainties of ref. 8 and 1-1/2% uncertainties on the $^{233}U/^{235}U$ ratio.

[d]Values obtained by spectrum stripping, see text.

Table 1-C, ^{235}U Inelastic Scattering

A	B	C	D	E	F	G	H
E_n (MeV)	E_x (MeV)	σ_t (b)[a]	σ_f (b)[b]	σ_c (b)[b]	σ_{scat} (b) = C-D-E	σ_{exp} (b)	σ_{inel} (b) = (F-G) x k[d]
0.93	$\geq$ 0.09	7.01 $\pm$ .105[a] (6.94)[b]	1.188 $\pm$ .030	0.121 $\pm$ .012	5.701 $\pm$ .110	5.02 $\pm$ .200 (5.00)[c]	0.662 $\pm$ .228 ($\pm$ 34%)
1.48	$\geq$ 0.18	6.83 $\pm$ .102[a] (6.78)[b]	1.249 $\pm$ .031	0.075 $\pm$ .008	5.506 $\pm$ .107	4.17 $\pm$ .125 (4.15)[c]	1.303 $\pm$ .164 ($\pm$ 12.6%)
1.50	$\geq$ 0.18	6.84 $\pm$ .103[a] (6.79)[b]	1.252 $\pm$ .031	0.075 $\pm$ .008	5.513 $\pm$ .108	4.28 $\pm$ .128 (4.26)[c]	1.194 $\pm$ .167 ($\pm$ 14.8%)
1.85	$\geq$ 0.18	7.10 $\pm$ .107[a] (7.04)[b]	1.291 $\pm$ 0.032	0.059 $\pm$ .006	5.750 $\pm$ .112	4.32 $\pm$ .129 (4.31)[c]	1.389 $\pm$ .171 ($\pm$ 12.9%)
2.48	$\geq$ 0.30	7.57 $\pm$ .114[a] (7.56)[b]	1.270 $\pm$ .038	0.042 $\pm$ .004	6.258 $\pm$ .120	4.70 $\pm$ .141 (4.67)[c]	1.516 $\pm$ .185 ($\pm$ 12.2%)
2.55	$\geq$ 0.30	7.60 $\pm$ .114[a] (7.60)[b]	1.263 $\pm$ .038	0.042 $\pm$ .004	6.295 $\pm$ .120	4.85 $\pm$ .146 (4.79)[c]	1.397 $\pm$ .189 ($\pm$ 13.5%)
3.48	$\geq$ 0.30	7.95 $\pm$ .119[a] (7.93)[b]	1.176 $\pm$ .035	0.029 $\pm$ .0029	6.745 $\pm$ .124	5.37 $\pm$ .164 (5.34)[c]	1.323 $\pm$ .206 ($\pm$ 15.6%)
3.55	$\geq$ 0.30	7.96 $\pm$ .119[a] (7.93)[b]	1.169 $\pm$ .035	0.029 $\pm$ .0029	6.762 $\pm$ .124	5.11 $\pm$ .153 (5.10)[c]	1.615 $\pm$ .196 ($\pm$ 12.1%)

[a]Taken from W. Poenitz et al., ref. 7.

[b]Taken from ENDF/B-V, ref. 8.

[c]Taken from stripped spectra, see text.

[d]"k" is the correction for ^{238}U content of the sample.

Table 1-D, ^{238}U Inelastic Scattering

A	B	C	D	E	F	G	H
E_n (MeV)	E_x (MeV)	σ_t (b)	σ_f (b)[c]	σ_c (b)[b]	σ_{scat} (b) = C-D-E	σ_{exp} (b)	σ_{inel} (b) = F-G
0.93	$\geq$ 0.09	7.21 $\pm$ .108[a] (7.18)[b]	0.0166 $\pm$ .001	0.125 $\pm$ .012	7.068 $\pm$ .109	6.12 $\pm$ .240	0.948 $\pm$ .263 ($\pm$ 27%)
1.48	$\geq$ 0.18	7.04 $\pm$ .106[a] (6.99)[b]	0.330 $\pm$ .010	0.057 $\pm$ .006	6.653 $\pm$ .107	4.62 $\pm$ .138 (4.61)[d]	2.033 $\pm$ .174 ($\pm$ 8.6%)
1.50	$\geq$ 0.18	7.05 $\pm$ .106[a] (7.00)[a]	0.347 $\pm$ .010	0.057 $\pm$ .006	6.646 $\pm$ .107	4.66 $\pm$ .139 (4.65)[d]	1.986 $\pm$ .175 ($\pm$ 8.8%)
1.85	$\geq$ 0.18	7.23 $\pm$ .108[a] (7.198)[a]	0.504 $\pm$ .006	0.048 $\pm$ .005	6.678 $\pm$ .108	4.39 $\pm$ .132	2.288 $\pm$ .171 ($\pm$ 7.5%)
2.48	$\geq$ 0.20	7.60 $\pm$ .114[a] (7.632)[a]	0.539 $\pm$ .016	0.028 $\pm$ .003	7.033 $\pm$ .115	4.54 $\pm$ .136 (4.54)[d]	2.493 $\pm$ .178 ($\pm$ 7.1%)
2.55	$\geq$ 0.20	7.63 $\pm$ .114[a] (7.678)[a]	0.538 $\pm$ .016	0.028 $\pm$ .003	7.064 $\pm$ .115	4.67 $\pm$ .140 (4.64)[d]	2.394 $\pm$ .181 ($\pm$ 7.5%)
3.48	$\geq$ 0.30	7.98 $\pm$ .120[a] (7.956)[a]	0.533 $\pm$ .013	0.015 $\pm$ .002	7.432 $\pm$ .121	5.24 $\pm$ .157 (5.25)[d]	2.192 $\pm$ .198 ($\pm$ 9.0%)
3.55	$\geq$ 0.30	7.99 $\pm$ .120[a] (7.970)[b]	0.536 $\pm$ .013	0.015 $\pm$ .002	7.439 $\pm$ .121	5.06 $\pm$ .151 (5.02)[d]	2.379 $\pm$ .193 ($\pm$ 8.1%)

[a]Taken from W. Poenitz et al., ref. 7.

[b]Taken from ENDF/B-V, ref. 8.

[c]Taken from ANL/NDM-32, ref. 2.

[d]Taken from stripped spectra, see text.

Table 1-E, ^{239}Pu Inelastic Scattering

A	B	C	D	E	F	G	H
E_n (MeV)	E_x (MeV)	σ_t (b)[a]	σ_f (b)[c]	σ_c (b)[b]	σ_{scat} (b) = C-D-E	σ_{exp} (b)	σ_{inel} (b) = F-G
0.93	$\geq$ 0.09	7.12 $\pm$ .107 (7.076)[a]	1.669 $\pm$ .048	0.029 $\pm$ .0029	5.42 $\pm$ .121	4.93 $\pm$ .246 (4.84)[d]	0.492 $\pm$ .274 ($\pm$ 55.7%)
1.48	$\geq$ 0.18	7.02 $\pm$ .106 (6.998)[a]	1.952 $\pm$ .052	0.013 $\pm$ .0013	5.06 $\pm$ .120	4.22 $\pm$ .127 (4.13)[d]	0.835 $\pm$ .174 ($\pm$ 20.8%)
1.50	$\geq$ 0.18	7.03 $\pm$ .105 (7.011)[a]	1.951 $\pm$ .059	0.013 $\pm$ .0013	5.07 $\pm$ .119	4.15 $\pm$ .124 (4.08)[d]	0.916 $\pm$ .172 ($\pm$ 18.8%)
1.85	$\geq$ 0.18	7.16 $\pm$ .107 (7.196)[b]	1.968 $\pm$ .056	0.0092 $\pm$ .0009	5.18 $\pm$ .121	4.11 $\pm$ .123 (3.97)[d]	1.073 $\pm$ .172 ($\pm$ 16.0%)
2.48	$\geq$ 0.30	7.55 $\pm$ .113 (7.621)[b]	1.892 $\pm$ .051	0.0048 $\pm$ .0005	5.65 $\pm$ .124	4.43 $\pm$ .133 (4.26)[d]	1.223 $\pm$ .182 ($\pm$ 14.9%)
2.55	$\geq$ 0.30	7.59 $\pm$ .113 (7.659)[b]	1.895 $\pm$ .051	0.0048 $\pm$ .0005	5.69 $\pm$ .124	4.74 $\pm$ .142 (4.46)[d]	0.950 $\pm$ .188 ($\pm$ 19.9%)
3.48	$\geq$ 0.30	7.95 $\pm$ .119 (7.975)[b]	1.825 $\pm$ .049	0.0024 $\pm$ .0002	6.12 $\pm$ .128	5.45 $\pm$ .163 (5.28)[d]	0.673 $\pm$ .208 ($\pm$ 30.9%)
3.55	$\geq$ 0.30	7.96 $\pm$ .119 (7.976)[b]	1.814 $\pm$ .049	0.0024 $\pm$ .0002	6.14 $\pm$ .128	5.10 $\pm$ .153 (4.98)[d]	1.040 $\pm$ .198 ($\pm$ 19.1%)

[a]Taken from W. Poenitz et al., ref. 7.

[b]Taken from ENDF/B-V, ref. 8.

[c]Taken from the $^{239}Pu/^{235}U$ ratio values of ref. 18 and the ^{235}U values of ENDF/B-V, ref. 8.

[d]Taken from stripped spectra, see text.

Table 1-F, ^{240}Pu Inelastic Scattering

A	B	C	D	E	F	G	H
E_n (MeV)	E_x (MeV)	σ_t (b)[a]	σ_f (b)[b]	σ_c (b)[c]	σ_{scat} (b) = C-D-E	σ_{exp} (b)	σ_{inel} (b) = F-G
1.48	$\geq$ 0.18	6.90 $\pm$ .09 (6.94)[c]	1.553 $\pm$ .043	0.073 $\pm$ .007	5.274 $\pm$ .100	4.363 $\pm$ .131 (4.226)[d]	0.911 $\pm$ .167 ($\pm$ 18.0%)
1.50	$\geq$ 0.18	6.91 $\pm$ .09 (6.95)[c]	1.553 $\pm$ .043	0.073 $\pm$ .007	5.284 $\pm$ .100	4.325 $\pm$ .130	0.959 $\pm$ .164 ($\pm$ 17.1%)
1.85	$\geq$ 0.18	7.15 $\pm$ .11 (7.14)[c]	1.645 $\pm$ .045	0.058 $\pm$ .006	5.447 $\pm$ .119	4.257 $\pm$ .127 (4.171)[d]	1.190 $\pm$ .174 ($\pm$ 14.6%)
2.48	$\geq$ 0.30	7.50 $\pm$ .11 (7.55)[c]	1.677 $\pm$ .038	0.039 $\pm$ .004	5.784 $\pm$ .116	4.579 $\pm$ .138 (4.449)[d]	1.205 $\pm$ .180 ($\pm$ 14.9%)
2.55	$\geq$ 0.30	7.57 $\pm$ .11 (7.59)[c]	1.673 $\pm$ .038	0.039 $\pm$ .004	5.858 $\pm$ .116	4.760 $\pm$ .143	1.098 $\pm$ .184 ($\pm$ 16.8%)
3.48	$\geq$ 0.35	7.99 $\pm$ .14 (7.95)[c]	1.676 $\pm$ .046	0.023 $\pm$ .002	6.291 $\pm$ .147	5.170 $\pm$ .155 (5.110)[d]	1.121 $\pm$ .213 ($\pm$ 19.0%)
3.55	$\geq$ 0.35	8.00 $\pm$ .14 (7.95)[c]	1.669 $\pm$ .046	0.023 $\pm$ .002	6.308 $\pm$ .147	4.920 $\pm$ .147	1.388 $\pm$ .207 ($\pm$ 14.9%)

[a]Taken from W. Poenitz et al., ref. 7.

[b]$^{240}Pu/^{235}U$ fission ratios from ref. 19 and ^{235}U fission cross sections from ENDF/B-V, ref. 8.

[c]Taken from ENDF/B-V, ref. 8.

[d]Values obtained by spectrum stripping as described in the text.